Analysis and Optimization of a New Differentially Driven Cable Parallel Robot

Hamed Khakpour
Mechanical Engineering Department,
Ecole Polytechnique of Montreal,
Montreal, QC H3T 1J4, Canada
e-mail: hamed.khakpour@polymtl.ca

Lionel Birglen
Mechanical Engineering Department,
Ecole Polytechnique of Montreal,
Montreal, QC H3T 1J4, Canada
e-mail: lionel.birglen@polymtl.ca

Souheil-Antoine Tahan
Mechanical Engineering Department,
Ecole de technologie superieure,
Montreal, QC H3C 1K3, Canada
e-mail: antoine.tahan@etsmtl.ca

In this paper, a new three degrees of freedom (DOF) differentially actuated cable parallel robot is proposed. This mechanism is driven by a prismatic actuator and three cable differentials. Through this design, the idea of using differentials in the structure of a spatial cable robot is investigated. Considering their particular properties, the kinematic analysis of the robot is presented. Then, two indices are defined to evaluate the workspaces of the robot. Using these indices, the robot is subsequently optimized. Finally, the performance of the optimized differentially driven robot is compared with fully actuated mechanisms. The results show that through a proper design methodology, the robot can have a larger workspace and better performance using differentials than the fully driven cable robots using the same number of actuators. [DOI: 10.1115/1.4028931]

Keywords: cable robot, differential mechanism, kinematic analysis, workspace, optimization

1 Introduction

Cable-driven manipulators are a particular class of parallel mechanisms where the moving platform (MP) is connected to the base platform (BP) through a set of cables [1]. Compared to linkage-driven designs, cable robots are usually less expensive, simpler, lighter, have low friction/inertia, and larger workspace [2–7]. On the other hand, they suffer from the unilateral and limited force in the cables, are prone to vibrations, and the possibility of interferences among cables. These issues can weaken their capability to be used in some applications [3,4,8].

Since cables are flexible, they can only sustain tension but not compression [8]. Thus, n-DOF cable-driven robots should have at least $n+1$ cables to fully constrain and manipulate the MP [2,9,10]. It should be noted that, using more cables, one can expect better performance and larger workspace for these mechanisms as reported in the literature [6,8].

Previously, different properties of cable-driven mechanisms such as wrench closure and wrench feasible workspaces (WCW and WFW), arrangement and interference of cables were at the center of attention of many research initiatives. For instance, Fattah and Agrawal [8] proposed a method for the optimal design of a cable-suspended planar robot, in which the global dexterity index (GDI) and the area of the workspace were used as indices to optimize the number of cables, size, and geometry of the MP. Shiang et al. [11] analyzed the kinematic properties of a 3DOF cable-suspended crane. In this study, the flexibility of cables was considered to obtain the equations of motion. Gouttefarde and Gosselin [7] developed an algorithm to find the WC and reachable workspaces of a planar cable robot. Also, Bouchard et al. [1] introduced a geometrical approach to investigate the WF property of cable robots with two to six DOFs.

With all these robots, an actuation redundancy is necessary, which significantly increases the cost and makes it harder to control the robots. In general, since the performances of these mechanisms are improved by employing more cables, these drawbacks become a painful burden. To overcome this issue, in this paper, a new 3DOF cable-driven mechanism is proposed in which the MP is manipulated by three differentials instead of a set of independently actuated cables. The idea of using cable differentials in the structure of a planar cable robot was presented and investigated by the authors in Ref. [12]. Although, a closely related design to differentially driven cable robots has been presented in Ref. [13], it was only one example of a much larger family of architectures based on differentials as proposed in Ref. [12]. In this paper, the impact of cable differentials on the performance of a spatial architecture is analyzed. The differentials considered in this paper are composed of two cables simultaneously driven by a single actuator through a differential mechanism. As described in Ref. [12] for planar cases, this technique can be generalized by using diverse numbers of cables with different arrangements while few actuators are considered. Through the comparison of this differentially driven mechanism with fully actuated solutions the authors reveal that by using differentials in the structure of this robot, its performances are improved.

2 A New Differentially Driven Cable Robot

Differentials are widely used in many mechanical devices to resolve an actuation source into two outputs or combine two inputs into a single output. By definition, they have 2DOF [14,15]. Commonly used examples of these mechanisms are bevel gear differentials, planetary gear differential, seesaw mechanisms, and tendon–pulley arrangements [16].

The difference between differentially actuated cables and independently driven ones was investigated for a two cables system by the authors in Ref. [12]. It was shown that the cables of the differential system have dependent forces (with ideally equal magnitude). Thus, as depicted in Fig. 1, their resultant force lies on a particular line (ideally again, on the bisector of the two cables). This property can be beneficial in the design of cable manipulators.

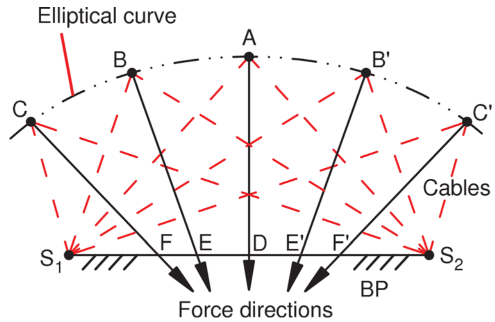

Fig. 1 Direction of resultant force of the two cables of a differential when its actuator is locked

Manuscript received August 29, 2013; final manuscript received October 18, 2014; published online June 10, 2015. Assoc. Editor: Xilun Ding.

As illustrated in Fig. 1, when the attachments point of the cables on the MP lies on point A (equidistant of points S_1 and S_2), the direction of this force passes though the midpoint of line S_1S_2. Then, this system acts as a single cable connected at points A and D. On the other hand, if this attachment point moves away from point A (e.g., toward points B or C), the bisector of the two cables crosses the line S_1S_2 at points different than the midpoint D (e.g., points E or F). This gives a unique property to differentials when they are used in the structure of a cable driven robot, namely, to have variable virtual attachment points on the BP.

The objective in designing a differentially driven cable robot is to use differentially driven cables in its architecture to fully constrain its MP while the number of the actuators is kept at minimum and more cables are used. In the presented mechanism, an actuated prismatic joint similar to the one presented in Ref. [17] is used to increase the stiffness of the robot and maintain the cable tensions. As illustrated in Fig. 2, this robot is cylindrically symmetric and the prismatic joint is connected to the BP through a passive universal joint. It is then rigidly connected to the MP in order for this robot to have 3DOF. The cables of the three differentials are connecting the three vertices of the triangular MP to the virtual cylindrical surface on the BP along three parallel lines. Consequently, the robot has four actuators (three in the differentials and one in the prismatic joint) and is redundant.

In this robot, there are seven connections between the MP and the BP, namely, a prismatic joint and six cables. These cables are driven by three differentials embedded in the BP at points $S_1 - S_2, S_3 - S_4$, and $S_5 - S_6$, so that point P_i is connected to points S_{2i-1} and S_{2i} via the cables $2i-1$ and $2i$. Note that the reason to select these pairs of cables to be differentially driven is to maximize certain characteristics (which will be specified later) related to the performance of this robot. Nevertheless, other pair of cables can also be chosen but the resulting performance would be actually weakened. The schematics of one of these three identical single differentials and its bevel gear mechanism are illustrated in Fig. 3. As can be seen in this figure, each differential has a single actuator installed in the BP and drives the two cables through a bevel gear differential mechanism while the other sides of the cables are attached to the MP. These three mechanisms are here referred to as $S_1 - P_1 - S_2, S_3 - P_2 - S_4$, and $S_5 - P_3 - S_6$. It should be noted that the introduced differential can also be replaced by other types of differentials, which are not considered in this paper (see Ref. [12]).

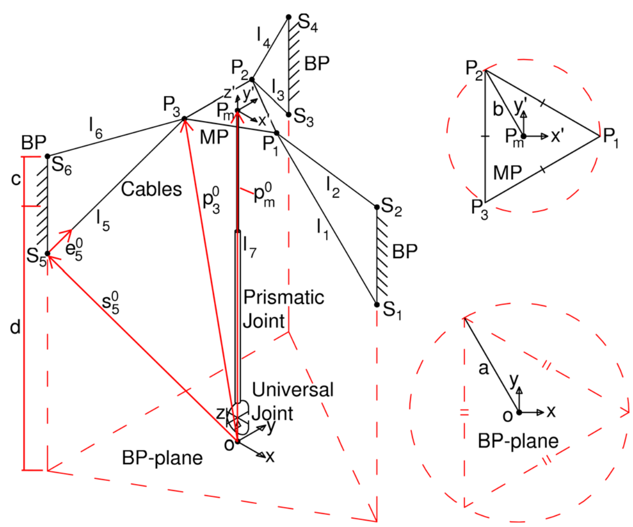

Fig. 2 Schematic of the proposed 3DOF differentially driven cable robot

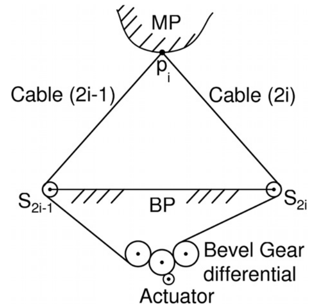

Fig. 3 Schematic of a differentially actuated cable system

3 Kinematic Analysis of the Robot

3.1 Inverse Kinematic Problems (IKPs). To solve the IKP of the robot, the position vectors of the attachment points of the cables on the BP with respect to the inertial frame (centered in O, cf. Fig. 2), $\mathbf{s}_j^0$ for $j = 1, \ldots, 6$, and on the MP with respect to the local frame (centered in P_m, cf. Fig. 2), $\mathbf{p}_i^m$ for $i = 1, 2, 3$, are considered. Then, the positions of points P_i^0 with respect to the inertial frame are found as

$$\mathbf{p}_i^0 = \mathbf{R}_m^0 \mathbf{p}_i^m + \mathbf{p}_m^0 \quad \text{for} \quad i = 1,\ 2,\ 3 \tag{1}$$

where $\mathbf{p}_m^0 = [x, y, z]$ is the position vector of the center of the MP and $\mathbf{R}_m^0$ is the rotation matrix of the later expressed as $\mathbf{R}_m^0 = \mathbf{R}_x(\theta_1)\mathbf{R}_y(\theta_2)$, where $\mathbf{R}_x(\theta_1)$ and $\mathbf{R}_y(\theta_2)$ are, respectively, the rotation matrix around the x-axis of the inertial frame with an angle θ_1, and then, around the y-axis, with an angle θ_2, of the resulting frame attached to the universal joint.

By considering $\mathbf{e}_j$ for $j = 1, \ldots, 6$ as unit vectors along the cables from S_j to P_i defined in the inertial frame, and also knowing the position vector $\mathbf{p}_m^0$, the IKP is solved as

$$\theta_1 = -a\tan 2(z, y) \quad \text{where} \quad \theta_1 \in [-\pi, \pi] \tag{2a}$$

$$\theta_2 = \arcsin\left(\frac{x}{l_7}\right) \quad \text{where} \quad \theta_2 \in \left[-\frac{\pi}{2}, \frac{\pi}{2}\right] \tag{2b}$$

$$l_j = \left\| \mathbf{s}_j^0 - \mathbf{p}_i^0 \right\| \quad \text{for} \begin{cases} j = 1,2 & \text{if} \quad i = 1 \\ j = 3,4 & \text{if} \quad i = 2 \\ j = 5,6 & \text{if} \quad i = 3 \end{cases} \quad \text{and} \quad l_7 = \left\| \mathbf{p}_m^0 \right\| \tag{2c}$$

$$l_{a1} = l_1 + l_2, \quad l_{a2} = l_3 + l_4, \quad l_{a3} = l_5 + l_6 \tag{2d}$$

where l_7 is the length of the prismatic joint, l_j for $j = 1, \ldots, 6$ is the length of the jth cable and l_{ai} for $i = 1, 2, 3$ is the total length of the cables driven by the ith differential. To solve the direct kinematic problem of the robot a numerical method such as a gradient descend method can be used.

3.2 Direct and Inverse Velocity Problems (IVPs). To obtain the relationships between the twist of the MP and the actuated joint rates, the Jacobian matrix of the robot must be defined. This matrix can be readily obtained by taking the derivatives of the position vectors $\mathbf{p}_i^0$. Knowing the twist of the MP at the point P_m, the IVP of this mechanism is solved as

$$\begin{bmatrix} \dot{l}_1 \\ \dot{l}_2 \\ \dot{l}_3 \\ \dot{l}_4 \\ \dot{l}_5 \\ \dot{l}_6 \\ \dot{l}_7 \end{bmatrix} = \begin{bmatrix} \mathbf{e}_1^{\mathrm{T}} & (\mathbf{p}_1^0 \times \mathbf{e}_1)^{\mathrm{T}} \\ \mathbf{e}_2^{\mathrm{T}} & (\mathbf{p}_1^0 \times \mathbf{e}_2)^{\mathrm{T}} \\ \mathbf{e}_3^{\mathrm{T}} & (\mathbf{p}_2^0 \times \mathbf{e}_3)^{\mathrm{T}} \\ \mathbf{e}_4^{\mathrm{T}} & (\mathbf{p}_2^0 \times \mathbf{e}_4)^{\mathrm{T}} \\ \mathbf{e}_5^{\mathrm{T}} & (\mathbf{p}_3^0 \times \mathbf{e}_5)^{\mathrm{T}} \\ \mathbf{e}_6^{\mathrm{T}} & (\mathbf{p}_3^0 \times \mathbf{e}_6)^{\mathrm{T}} \\ \mathbf{e}_7^{\mathrm{T}} & \mathbf{0}_{1\times 3} \end{bmatrix} \begin{bmatrix} \mathbf{v}^{\parallel} \\ \omega \end{bmatrix} \leftrightarrow \dot{\mathbf{l}} = \mathbf{J}\mathbf{t} \tag{3}$$

where $\dot{l}_j$ for $j = 1, ..., 7$ are the length change rates of the six cables and the prismatic joint; $\dot{\mathbf{l}}$ is the vectors of the joint rates and $\mathbf{t} = \begin{bmatrix} \mathbf{v}^{\parallel} \\ \omega \end{bmatrix}$; $\mathbf{v}$ and ω are, respectively, the linear and angular velocity vectors of the MP at the point P_m and $\mathbf{v}^{\parallel} = \mathbf{e}_7\mathbf{e}_7^{\mathrm{T}}\mathbf{v}$. Since the robot only has 3DOF, the vectors $\mathbf{v}$ and ω are related. To find this, by projecting the vector $\mathbf{v}$ onto a plane with normal of $\mathbf{e}_7$ and calculating the derivative of position vector $\mathbf{p}_m = l_7\mathbf{e}_7$, the passive joint rates (in the universal joint) are obtained as

$$\dot{\theta}_1 = \frac{\dfrac{-v_y^{\perp}}{l_7} + \dot{\theta}_2 s_{\theta_1} s_{\theta_2}}{c_{\theta_1} c_{\theta_2}} \quad \text{and} \quad \dot{\theta}_2 = \frac{v_x^{\perp}}{l_7 c_{\theta_2}} \tag{4}$$

where $v_x^{\perp}$ and $v_y^{\perp}$, respectively, denote x and y components of the vector $\mathbf{v}^{\perp} = (\mathbf{I}_{3\times 3} - \mathbf{e}_7\mathbf{e}_7^{\mathrm{T}})\mathbf{v}$. Next, the angular velocity is found as

$$\omega = \begin{bmatrix} \dot{\theta}_1 \\ \dot{\theta}_2 c_{\theta_1} \\ \dot{\theta}_2 s_{\theta_1} \end{bmatrix} \tag{5}$$

The linear velocities of the actuators of the differentials (i.e., the displacement rates of the two cables of each differential) are then found as $\dot{\mathbf{l}}_a = \mathbf{T}\dot{\mathbf{l}}$ where $\dot{\mathbf{l}}_a = [\dot{l}_{a1} \;\; \dot{l}_{a2} \;\; \dot{l}_{a3} \;\; \dot{l}_7]^{\mathrm{T}}$ is the vector of actuation rates and matrix $\mathbf{T}$ is found from Eq. (2*d*) as

$$\mathbf{T} = \begin{bmatrix} 1 & 1 & 0 & 0 & 0 & 0 & 0 \\ 0 & 0 & 1 & 1 & 0 & 0 & 0 \\ 0 & 0 & 0 & 0 & 1 & 1 & 0 \\ 0 & 0 & 0 & 0 & 0 & 0 & 1 \end{bmatrix} \tag{6}$$

Finally, the IVP can be solved as

$$\begin{bmatrix} \dot{l}_{a1} \\ \dot{l}_{a2} \\ \dot{l}_{a3} \\ \dot{l}_7 \end{bmatrix} = \begin{bmatrix} \mathbf{e}_1^{\mathrm{T}} + \mathbf{e}_2^{\mathrm{T}} & (\mathbf{p}_1^0 \times (\mathbf{e}_1 + \mathbf{e}_2))^{\mathrm{T}} \\ \mathbf{e}_3^{\mathrm{T}} + \mathbf{e}_4^{\mathrm{T}} & (\mathbf{p}_2^0 \times (\mathbf{e}_3 + \mathbf{e}_4))^{\mathrm{T}} \\ \mathbf{e}_5^{\mathrm{T}} + \mathbf{e}_6^{\mathrm{T}} & (\mathbf{p}_3^0 \times (\mathbf{e}_5 + \mathbf{e}_6))^{\mathrm{T}} \\ \mathbf{e}_7^{\mathrm{T}} & \mathbf{0}_{1\times 3} \end{bmatrix} \begin{bmatrix} \mathbf{v}^{\parallel} \\ \omega \end{bmatrix} \tag{7}$$

The first matrix in the right hand side of Eq. (7) is referred to as a modified Jacobian, $\mathbf{J}_m$, particular to the proposed differential cable-driven robot.

The direct velocity problem (DVP) aims at finding the twist of the MP when the joint rates are known. Considering Eqs. (4), (5), and (7) and knowing the configuration of the robot, there are four equations and three unknowns (i.e., the components of $\mathbf{v}$). Therefore, if one of these equations is dependent to the others then there is a solution, otherwise, that vector of joint rates $\dot{\mathbf{l}}$ is deemed not feasible.

3.3 Actuation Forces and Output Wrench Relationships.

The tension matrix of a cable robot is defined as $\mathbf{A} = \mathbf{J}^{\mathrm{T}}$ [8]. Using the principle of virtual work the relationship between the forces in the cables and the prismatic joint of the robot and the corresponding wrench at its MP is

$$\mathbf{A}\mathbf{f} = \mathbf{w} \tag{8}$$

where $\mathbf{f}$ and $\mathbf{w}$ are, respectively, the vectors describing the tension forces and the wrench. They are defined as

$$\mathbf{f} = \begin{bmatrix} t_1 & t_2 & t_3 & t_4 & t_5 & t_6 & t_7 \end{bmatrix}^{\mathrm{T}} \quad \text{and} \quad \mathbf{w} = \begin{bmatrix} \mathbf{f}_w^{\mathrm{T}} & \mathbf{n}_w^{\mathrm{T}} \end{bmatrix}^{\mathrm{T}} \tag{9}$$

where t_j for $j = 1, \cdots, 6$ is the magnitude of the force in the jth cable and t_7 is the magnitude of the force in the prismatic joint. Also, $\mathbf{f}_w$ and $\mathbf{n}_w$ are, respectively, the vectors of force and torque exerted to the MP at the point P_m. In a frictionless ideal case, the bevel gear system can produce equal tensions on both cables in each differential, i.e., $t_1 = t_2, t_3 = t_4$, and $t_5 = t_6$. Consequently, vector $\mathbf{f}$ can be changed to $\mathbf{f} = \begin{bmatrix} t_1 & t_1 & t_3 & t_3 & t_5 & t_5 & t_7 \end{bmatrix}^{\mathrm{T}}$.

The total torque to be generated by the actuators of the differentials are $\tau_{a1} = 2r_g t_1, \tau_{a2} = 2r_g t_3$, and $\tau_{a3} = 2r_g t_5$, where r_g is the gear ratio. Additionally, with this robot, the resultant force of the cables of each differential is considered to characterize its performance. Therefore, similar to the velocity problem and using the modified Jacobian, Eq. (8) is changed to

$$\mathbf{A}_m\mathbf{f}_m = \mathbf{w} \tag{10}$$

where $\mathbf{A}_m = \mathbf{J}_m^{\mathrm{T}}$ and $\mathbf{f}_m = [t_1 \;\; t_3 \;\; t_5 \;\; t_7]^{\mathrm{T}}$. This robot is a 3DOF mechanism (with two rotations and one translation) and works in a three dimensional space. On the other hand, an external wrench imposed to this robot as well as the resultant force and torque generated by the three differentials and the prismatic joint can have arbitrary directions. Indeed, considering the constraint exerted by the universal joint to the MP, the wrench that should be resisted by the actuators is limited to a force in the direction of $\mathbf{e}_7$ and a torque on a plane created by two cross axes of the universal joint with a normal defined as $\mathbf{e}_{\mathrm{U}} = [0 - s\theta_1 c\theta_1]^{\mathrm{T}}$ [18]. Therefore, to eliminate the components of the force and torque vectors which are passively resisted by the universal joint not the actuators, they are projected to the relevant directions using the matrix $\mathbf{C}$ defined as

$$\mathbf{C} = \begin{bmatrix} \mathbf{e}_7\mathbf{e}_7^{\mathrm{T}} & \mathbf{0}_{3\times 3} \\ \mathbf{0}_{3\times 3} & \mathbf{I}_{3\times 3} - \mathbf{e}_{\mathrm{U}}\mathbf{e}_{\mathrm{U}}^{\mathrm{T}} \end{bmatrix}_{6\times 6} \tag{11}$$

Then, if the vector $\mathbf{f}_m$ is known, by using the matrix $\mathbf{C}$, the left hand side of Eq. (10) is projected onto the specific directions so that the vector $\mathbf{w}$, which is not compensated by the passive reaction of the universal joint is found as

$$\mathbf{C}\mathbf{A}_m\mathbf{f}_m = \mathbf{w} \tag{12}$$

On the other hand, if an arbitrary external wrench vector, $\mathbf{w}_a$, is exerted to the MP and the vector $\mathbf{f}_m$ is to be found, this wrench should be first mapped into the directions controlled by the actuators, namely,

$$\mathbf{A}_m\mathbf{f}_m = \mathbf{C}\mathbf{w}_a \tag{13}$$

In Eqs. (12) and (13), the projection matrix $\mathbf{C}$ is used to take into account the components of the vectors of these equations in the actuated directions. Thus, one cannot compute any of these equations from the other. Any vector which has the same component in these directions would be a possible solution for these equations (either the generated wrench on the MP on the right hand side of Eq. (12) or the cable tensions in the left hand side of Eq. (13)). The other components of these vectors are resisted by the passive support of the robot.

Finding the resultant wrench using Eq. (12) is straightforward while in Eq. (13), there appears to be six equations and four variables. However, due to the constraints of the robot, there are only three independent equations. Therefore, this is an underdetermined system of equations. To solve this problem the WF condition is used. In this approach, it is assumed that one of the variables is known. Then, the three other variables are parametrically calculated. Next, the minimal and maximal allowed tensions in the cables are considered so that the minimum value is set for a cable which has the lowest tension while the tensions of the others should not exceed the maximum value. If such a force vector $\mathbf{f}_m$ is found, then, that wrench can be resisted by this robot.

3.4 Workspace of the Robot. Usually in the literature, two types of workspaces are defined for a cable-driven robot, i.e., the WCW and WFW [4]. The WCW is a volume where the MP of the robot can be located and regardless of the exerted wrench, all its cables are in tension. The WFW is where all cable tensions are within a specified range.

To find the WCW of the proposed robot, the distribution of the forces and torques produced by the actuators onto its MP must be investigated. These force/torque vectors should be able to span all directions in the considered n-D force/torque workspace to be able to produce any arbitrary wrench. To evaluate this for the forces, the unit vectors along the resultant force vector created by each differential at the MP and the prismatic joint (which can be either under compression or tension) are considered. Then, they are used to find the unit vectors along the corresponding torque vectors. Afterwards, a procedure similar to the one introduced in Ref. [4] is used to evaluate the WC condition in both force and torque spaces. Finally, if this condition is simultaneously satisfied for both the force and torque vectors then, that configuration belongs to the WCW of this robot.

To obtain the WFW, the tensions of all cables are desired to be between $t_{\min}$ and $t_{\max}$ and then, a geometrical method similar to the one proposed in Ref. [1] is used. This procedure is again implemented separately for the force and the torque vectors. Finally, for each pose, if the magnitude of both force and torque which can be exerted by the actuators to the MP are larger than their specified minimally allowable values, then that pose belongs to the WFW of the robot.

4 Defining the Characteristic Indices

The proposed robot is assumed to work in a cylindrical workspace with a radius r_c and a height h_c. The base of this cylinder is parallel to the BP plane and is located at a distance d_c from it. To optimize the performance of this robot, different aspects of its performance should be measured. In this paper, two measures are taken into account, namely, the size of the WCW and WFW. The investigation of these properties is performed via defining two dimensionless indices.

WCW: Evaluated by an index I_{WCW}. This index is defined as the ratio between the volume of the conceptual cylinder and the sum of the volumes of this cylinder and the WCW of the robot, namely,

$$I_{\mathrm{WCW}} = \frac{c}{c+q} \tag{14}$$

where c and q are the volume of, respectively, the cylinder and the WCW.

WFW: Measured by the index I_{WFW}, which is defined as

$$I_{\mathrm{WFW}} = \frac{c}{c+m}\left(\frac{f_{\min}}{f_{\min}+\frac{1}{m}\int_m f_i dv} + \frac{n_{\min}}{n_{\min}+\frac{1}{m}\int_m n_i dv}\right) \tag{15}$$

where m is the volume of the WFW; f_i and n_i are, respectively, the maximum feasible force and torque for each position of the MP in the WFW; also, $f_{\min}$ and $n_{\min}$ are, respectively, the specified minimal amount of force and torque the robot should be able to resist inside its WFW. The terms inside the parentheses in Eq. (15) show the normalized ratios between $f_{\min}/n_{\min}$ and the average values of the maximum feasible force/torque inside the WFW. This index considers both the volume of the WFW and the magnitude of the maximal permissible force and torque for all points in this workspace.

5 Optimization and the Results

The main objective in the optimization of the robot is to improve the performance of its three differentials to have a larger workspace. For this, the two indices and the conceptual cylinder are used to obtain the best set of design parameters. With this robot, the dimensions of the BP, i.e., a and d are assumed to be fixed while the dimension of the MP and the distance between two points of each differential (i.e., S_{2i-1} and S_{2i} for $i = 1, 2, 3$), respectively, b and c are to be found (c.f. Fig. 2). Considering the design limits of the robot, two boundaries are considered for these two goal parameters. In this process, the objective function to be minimized is defined as

$$F_{\mathrm{GA}} = a_1 I_{\mathrm{WCW}} + a_2 I_{\mathrm{WFW}} \tag{16}$$

where a_1 and a_2 are weight coefficients. The input parameters of the optimization procedure are the dimensions of the conceptual cylinder and the BP, the boundaries of the cables tensions and the force in the prismatic joint, and finally, the minimum amount of force and torque the robot should resist inside its WFW.

To optimize this robot, a genetic algorithm (GA), which is embedded in a commercial numerical software, is used. The chosen values of all input parameters and the boundaries are presented in Table 1.

Considering all these values, a GA with 120 individuals and 100 generations is run. The results of the optimization are presented in Table 2 and the schematic of the optimized robot in an arbitrary position inside its workspace is illustrated in Fig. 4.

As can be seen in Table 2, the GA found the best value for b exactly at the lower boundary. The same optimization with no boundary for b shows that this value is close to zero, which is physically impractical. The reason for this is that in the areas of the cylinder close to each of the differentials, with smaller value of b, there is a smaller angle between the cables of that differential and so these cables can produce larger resultant force. Thus, to get rid of this problem a minimum boundary is considered.

Finally, this optimization reveals that the effects of using differential in a cable robot is a trade off between the expansion of the range of changes in the direction of resultant force vector of each differential (which improves the both WCW and WFW) and the increase of the angle between their cables (which weakens the maximum value of the resultant force and so decreases the WFW).

Table 1 Values of all parameters used in the optimization process

Parameters	Values	Parameters	Values
a	60 cm	$t_{\min}$	10 N
d	90 cm	$t_{\max}$	100 N
r_c	40 cm	$t'_{\min}$	0 N
h_c	120 cm	$t'_{\max}$	600 N
d_c	30 cm	$f_{\min}$	400 N
		$n_{\min}$	90 N·m
a_1	3	Range for b	[5,30] cm
a_2	1	Range for c	[0,60] cm

Table 2 Resultants of the optimization process

Variables	Values	Dimensions
c	16.51	cm
b	5.00	cm

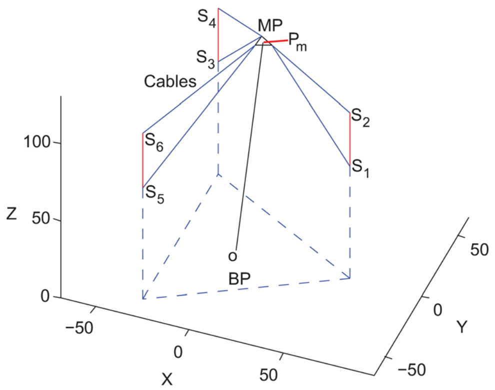

Fig. 4 Schematic of the optimized robot in an arbitrary location inside its workspace

6 Comparing the Proposed Differential Cable Robot With Two Fully Actuated Ones

In this section, to investigate the effect of using differentials in the structure of a cable robot, the optimized differentially actuated robot, referred to as 6-3-differential (with 6 cables and 3 actuators), is compared with two fully actuated designs. The first mechanism has an architecture similar to the proposed robot, but it is driven by three single cables instead of three differentials. The schematic of this robot, which is here referred to as 3-3-full, is illustrated in Fig. 5. The second fully actuated robot, called 6-6-full, has the same structure as the differential cable robot shown in Fig. 2, but all its cables are independently actuated.

This comparison is implemented for the two workspaces (WCW and WFW) of these robots. To do this, by taking the parameters of Tables 1 and 2, the indices I_{WCW} and I_{WFW} as well as the ratios between the volumes of these workspaces (i.e., respectively, v_{WCW} and v_{WFW}) and the volume of the cylinder v_{c} are measured and the results are presented in Table 3.

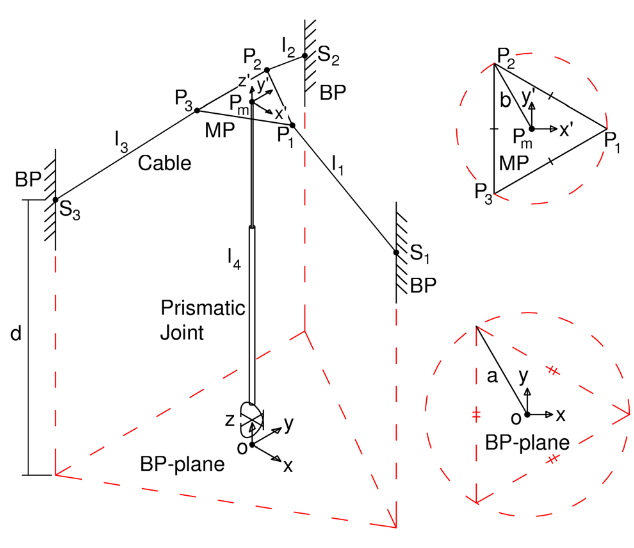

Fig. 5 Schematic of the 3-3-full cable robot with three independently actuated cables

Table 3 Comparing the performance of differential cable-driven robot with other mechanisms

	WCW		WFW	
Robot type	I_{WCW}	$v_{\mathrm{WCW}}/v_{\mathrm{c}}$	I_{WFW}	$v_{\mathrm{WFW}}/v_{\mathrm{c}}$
3-3-full cable robot	0.6194	0.6146	2	0
6-3-differential cable robot	0.6157	0.6241	0.8499	0.0705
6-6-full cable robot	0.5855	0.7081	0.8463	0.0731

As can be seen in this table, with the same values for the design parameters, the two indices of the 6-3-differential cable robot are smaller (i.e., better) than the ones of the 3-3-full mechanism. This means that using differentials, while the number of actuators is kept at minimum (three in this case) one can expect a larger WCW and WFW (which can also be seen as the ratios $v_{\mathrm{WCW}}/v_{\mathrm{c}}$ and $v_{\mathrm{WFW}}/v_{\mathrm{c}}$ in Table 3). This improvement is obtained as a result of two phenomena: first, the capability of using more cables with the same actuator via differentials; and second, the change in the direction of the resultant force of the cables of each differential (c.f. Fig. 1).

On the other hand, as one expected, these indices are even smaller with the 6-6-full robot than with the differentially actuated one. This shows that although the same number of cables is used in both architectures, due to the limits in the direction of the resultant force of the differentials, the 6-3-differential robot cannot have workspaces as large as the fully actuated one.

7 Conclusions

This paper proposed a new 3DOF cable parallel robot, which is actuated by differentials instead of independent cables. This robot has four actuators, one is a prismatic joint and three others are connected to three differentials to drive six cables. For this, first, the effects of using differentials on the forces exerted by the six cables on the MP were investigated. Next, the kinematic analysis of the robot was presented. Afterwards, to evaluate and optimize the two workspaces of the robot, the indices I_{WCW} and I_{WFW} were defined. Then, the workspaces of the optimized robot were compared with the ones of fully actuated mechanisms. The results showed that through a proper design and using differentials, the robot can have larger WCW and WFW with respect to the mechanism with the same number of actuators driving independent cables.

References

[1] Bouchard, S., Gosselin, C. M., and Moore, B., 2010, "On the Ability of a Cable-Driven Robot to Generate a Prescribed Set of Wrenches," ASME J. Mech. Rob., **2**(1), p. 011010.

[2] Perreault, S., and Gosselin, C. M., 2008, "Cable-Driven Parallel Mechanisms: Application to a Locomotion Interface," ASME J. Mech. Des., **130**(10), p. 102301.

[3] Tadokoro, S., Murao, Y., Hiller, M., Murata, R., Kohkawa, H., and Matsushima, T., 2002, "A Motion Base With 6-DOF by Parallel Cable Drive Architecture," IEEE ASME Trans. Mechatron., **7**(2), pp. 115–123.

[4] Yang, G., Pham, C. B., and Yeo, S. H., 2006, "Workspace Performance Optimization of Fully Restrained Cable-Driven Parallel Manipulators," IEEE International Conference on Intelligent Robots and Systems (IROS 2006), Beijing, China, Oct. 9–15, pp. 85–90.

[5] Ferlay, F., and Gosselin, F., 2008, "A New Cable-Actuated Haptic Interface Design," Haptics: Perception, Devices and Scenarios: 6th International Conference (EuroHaptics 2008), Madrid, Spain, June 10–13, pp. 474–483.

[6] Yang, G., Lin, W., Kurbanhusen, M. S., Pham, C. B., and Yeo, S. H., 2005, "Kinematic Design of a 7-DOF Cable-Driven Humanoid Arm: A Solution-in-Nature Approach," IEEE/ASME International Conference on Advanced Intelligent Mechatronics (AIM), Monterey, CA, July 24–28, pp. 444–449.

[7] Gouttefarde, M., and Gosselin, C. M., 2006, "Analysis of the Wrench-Closure Workspace of Planar Parallel Cable-Driven Mechanisms," IEEE Trans. Rob., **22**(3), pp. 434–445.

[8] Fattah, A., and Agrawal, S. K., 2005, "On the Design of Cable-Suspended Planar Parallel Robots," ASME J. Mech. Des., **127**(5), pp. 1021–1028.

[9] Kawamura, S., Choe, W., Tanaka, S., and Pandian, S. R., 1995, "Development of an Ultrahigh Speed Robot FALCON Using Wire Drive System," IEEE International Conference on Robotics and Automation (ICRA'95), Nagoya, Japan, May 21–27, pp. 215–220.

[10] Carricato, M., and Merlet, J. P., 2013, "Stability Analysis of Underconstrained Cable-Driven Parallel Robots," IEEE Trans. Rob., **29**(1), pp. 288–296.
[11] Shiang, W. J., Cannon, D., and Gorman, J., 2000, "Optimal Force Distribution Applied to a Robotic Crane With Flexible Cables," IEEE International Conference on Robotics and Automation (ICRA '00), San Francisco, CA, Apr. 24–28, pp. 1948–1954.
[12] Khakpour, H., Birglen, L., and Tahan, S. A., 2014, "Synthesis of Differentially Driven Planar Cable Parallel Manipulators," IEEE Trans. Rob., **3**(3), pp. 619–630.
[13] Liu, H., Gosselin, C., and Laliberte, T., 2012, "Conceptual Design and Static Analysis of Novel Planar Spring-Loaded Cable-Loop-Driven Parallel Mechanisms," AMSE J. Mech. Rob., **4**(2), p. 021001.
[14] IFToMM Commission A, 1991, "Terminology for the Theory of Machines and Mechanisms," Mech. Mach. Theory, **26**(5), pp. 435–539.
[15] Hirose, S., 1985, "Connected Differential Mechanism and Its Applications: Robotic Manipulator," International Conference on Advanced Robotics, Tokyo, Japan, Sept. 9–10, pp. 319–326.
[16] Birglen, L., Laliberte, T., and Gosselin, C., 2008, *Underactuated Robotic Hands*, Vol. 40, Springer-Verlag, New York.
[17] Landsberger, S., and Sheridan, T., 1987, "Parallel Link Manipulators," U.S. Patent No. 4,666,362.
[18] Carricato, M., and Gosselin, C., 2009, "On the Modeling of Leg Constraints in the Dynamic Analysis of Gough/Stewart-Type Platforms," ASME J. Comput. Nonlinear Dyn., **4**(1), p. 011008.